Decolorization of KN-R catalyzed by Fe-containing Y and ZSM-5 zeolites

Aiyin Chen, Xiaodong Ma, Hongwen Sun[*]

Key Laboratory of Environmental Pollution Process and Standard of Ministry of Education, College of Environmental Science and Engineering, Nankai University, 94 Weijin Road, Tianjin 300071, China

Abstract

Decolorization of an anthraquinone dye, Reactive Brilliant Blue KN-R by hydrogen peroxide was examined using Fe-containing Y and ZSM-5 zeolites as heterogeneous catalysts. Catalysts were prepared by ion-exchange and coprecipitation methods, and calcined at different temperatures. The surface morphologies, crystalline phases, and chemical-state of the catalysts were characterized by scanning electron microscopy, X-ray diffraction and X-ray photoelectron spectroscopy. Influences of reaction conditions, such as dye concentration, catalyst dosage and solution pH, were evaluated and the relations between catalytic capacity and surface microstructures were discussed. The results showed that Fe-containing Y and ZSM-5 zeolites generally exhibited similar or better catalytic efficiency compared with homogeneous Fenton reagent, with Fe-containing ZSM-5 being more efficient. Synthesis method and calcination temperature affected catalytic efficiency and the stability of catalysts. Fe-containing ZSM-5, which was prepared by coprecipitation and calcined at $450\,°C$, displayed the greatest decolorization capacity. Under the conditions of initial pH 2.5, $30.0\,mmol/L\ H_2O_2$ and $4.0\,g/L$ catalyst, $250\,mg/L$ KN-R could be decolorized over 90% within 20 min.
© 2008 Elsevier B.V. All rights reserved.

Keywords: Catalytic decolorization; Anthraquinone dye; Fe-containing zeolite; Heterogeneous Fenton-like oxidation

1. Introduction

Advanced oxidation techniques (AOTs), which can decompose or mineralize organic pollutants efficiently through generating highly oxidative radicals (such as $^\bullet OH$), are powerful technologies for treating wastewaters containing persistent organic pollutants. Among AOTs, Fenton oxidation which uses hydrogen peroxide as oxidant and Fe(II) ions as catalyst, has been widely applied in treating wastewaters containing organic pollutants [1,2]. But it has the shortcoming that Fe ions remain in the treated water, and additional step is needed to remove them. Efforts have been made to develop heterogeneous Fenton-like catalysts to overcome this shortcoming, which include supported Fe ions, clusters or oxides [3–10]. Mesoporous molecular sieves have drawn much attention due to their great surface area, high uniformity and easily controllable pore size. However, mesoporous molecular sieves have lower hydrothermal stability and mechanical strength than microporous zeolite-type molec-

ular sieves, their applications are hence limited in many cases [11,12]. Recently, several papers have reported that heterogeneous zeolite-based Fe catalysts, such as FeY and FeZSM-5, could provide similar catalytic activities as homogeneous Fe(II) ions [13–17]. However, their catalytic activity and stability depend much on synthesis methods in addition to their composition and framework structure. Moreover, leakage of iron ions from the supporter would result in new pollution of the treated water, which is an important factor that should be considered [18]. Till now, no systematical research has been conducted to confirm the actual heterogeneity of iron species supported on Y and ZSM-5 zeolites as heterogeneous Fenton-like catalysts.

Hence, in the present study, two types of Fe-containing catalysts were developed using ion-exchange and coprecipitation methods on Y and ZSM-5 zeolites, which have different framework structure. Their catalytic activity was examined by oxidation of a model organic pollutant (Reactive Brilliant Blue KN-R). The objectives of this study were to: (1) find the relationships between microstructural characteristics of the catalysts and their catalytic efficiency; (2) optimize reaction conditions of the heterogeneous Fenton-like oxidation and (3) investigate the leakage of iron ions in reactions to select more stable samples

---

[*] Corresponding author. Tel.: +86 22 23509241; fax: +86 22 23509241.
E-mail address: sunhongwen@nankai.edu.cn (H. Sun).

and minimize the possible secondary pollution of Fe-containing sludge.

2. Experimental

2.1. Materials and chemicals

The zeolites used in this study were NaY and ZSM-5 supplied by Heng-Ye Chemical Company (Shanghai, China). They were exchanged with 2 mol/L NH₄Cl for 12 h and calcinated at 400 °C for 2 h to activation [13,14]. Anthraquinone dye KN-R came from Tianjin Dye Chemical Company (Tianjin, China). Simulated dye wastewater was made up by dissolving specific amounts of KN-R in deionized water.

2.2. Synthesis and characterization

Fe-containing Y and ZSM-5 zeolites were synthesized using coprecipitation and ion-exchange methods [13–15]. In coprecipitation, $FeSO_4$ aqueous solution was adjusted to pH 4.0, and then zeolite powders were slowly added into the solution under stirring. After the suspension was subsequently stirred for 6 h, 20% $NH_3 \cdot H_2O$ solution was added drop by drop under stirring until the solution pH reached 9.0. The suspension was stirred for another 1 h. The precipitates were recovered by centrifugation, washed with deionized water for three times and dried at room temperature overnight. The supernate solutions of the first centrifugation and following washing were combined, and the amount of total iron ions in it was measured using 1,10-phenanthroline spectrophotometric method [19]. Iron-loading content on the catalysts was calculated through mass balance. The catalysts acquired by coprecipitation method are called $FeZSM-5_{co}$ and FeY_{co}, respectively. In ion-exchange, Na_2CO_3 powder was slowly added into $FeSO_4$ aqueous solution ([Fe]:[Na](mol/mol) = 1:1) under stirring, and then the solution was continuously stirred for 1 h. Subsequently, zeolite powders were slowly added in. Other procedures were the same. The catalysts acquired by ion-exchange are called $FeZSM-5_{ie}$ and FeY_{ie}, respectively. Parts of the finished catalysts were calcined for 2 h at 250, 350, 450 and 550 °C, respectively.

The crystalline structure of the catalyst was analyzed using a D/Max2500 X-ray diffractometer (Rigaku, Japan) with Cu Kα monochromatic radiation, operated at 40 kV and 100 mA. The microstructure at external surface of the catalysts was observed using an X-650 Scanning Electron Microscope (Hitachi, Japan). XPS spectra (X-ray photoelectron spectroscopy) were recorded using an Axis Ultra DLD spectrometer (Kratos, England) employing a monochromated Al-Ka X-ray source ($h\nu$=1486.6 eV), hybrid (magnetic/electrostatic) optics and a multi-channel plate and delay line detector (DLD). All XPS spectra were recorded using an aperture slot of $300 \times 700 \mu m$, survey spectra were recorded with a pass energy of 160 eV, and high-resolution spectra with a pass energy of 40 eV.

2.3. Decolorization of KN-R

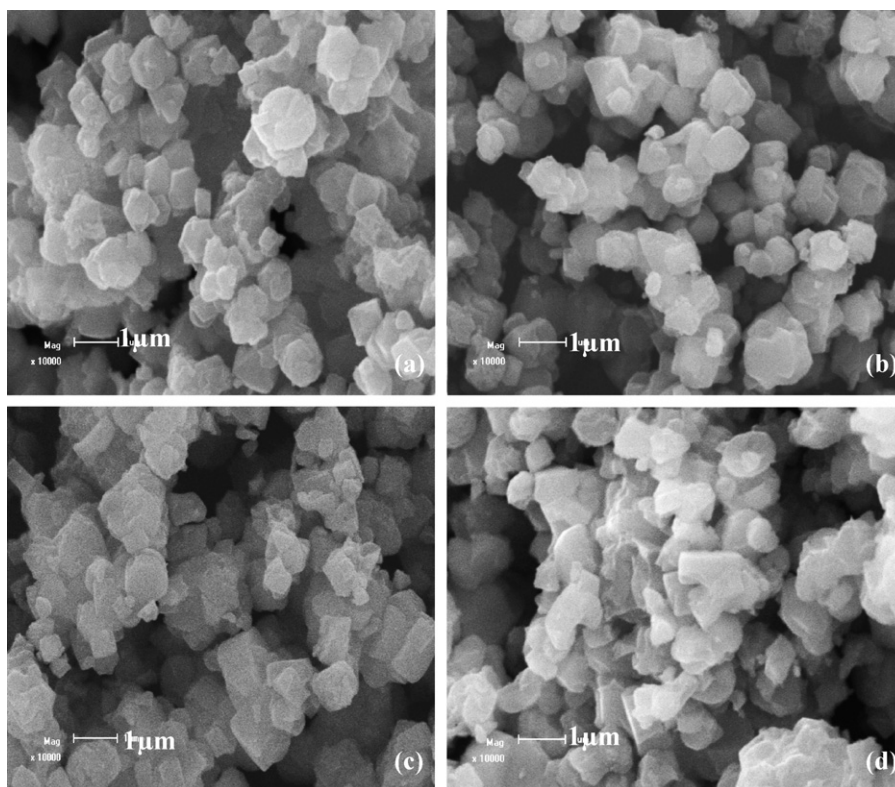Catalytic decolorization of KN-R was performed in 0.5 L aqueous solution containing 250 mg/L KN-R. Initial solution pH

Fig. 1. SEM micrographs of (a) FeY_{ie}, (b) FeY_{co}, (c) $FeZSM-5_{ie}$ and (d) $FeZSM-5_{co}$.
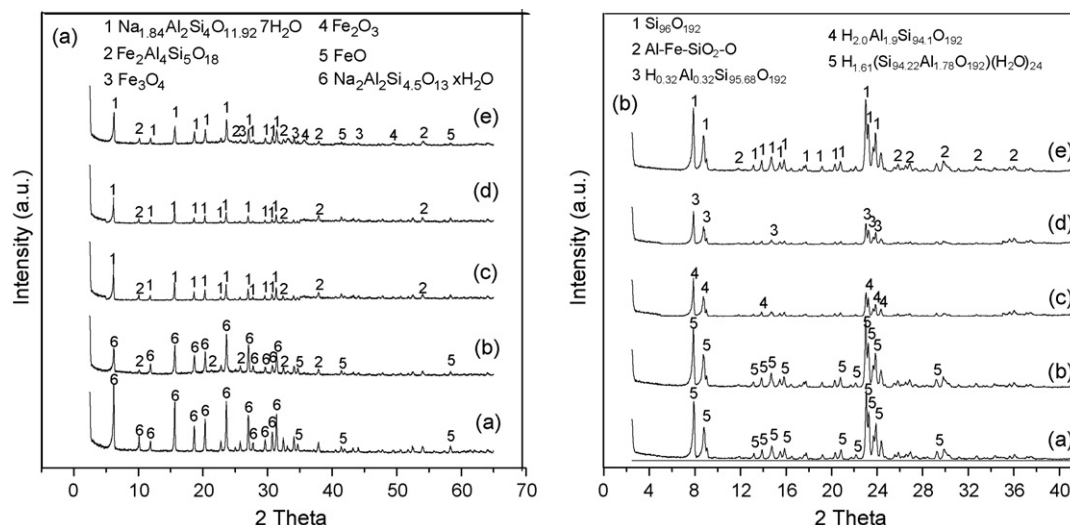
Fig. 2. XRD spectrogram of (a) FeY_{ie} and (b) $FeZSM-5_{co}$ (a–e represent the samples without calcination and calcined at 250, 350, 450 and 550 °C, respectively.).

was adjusted using 1.0 mol/L H_2SO_4 and NaOH. Four grams per liter catalysts were added into the solution followed by 50 mmol/L H_2O_2 to initiate the reaction. Electromagnetic stirring was applied during the reactions. Five milliliters suspension was taken out at designated times, and immediately amended with a few drops of 0.2 mol/L $Na_2S_2O_3$ to stop the reaction. The samples were centrifuged to remove the solid catalyst. Residue solution concentration of KN-R was measured using a UV-vis spectrophotometer (Model-UV752, Lei-Ci Precision & Scientific Instrument Company, Shanghai, China) at 594 nm. Fe (total iron ions) leaching during decolorization was measured using 1,10-phenanthroline method [19].

The experiments were repeated under different initial dye concentrations (250–500 mg/L), initial solution pHs (2.0–11.0), catalyst doses (2.0–8.0 g/L) and H_2O_2 doses (2–50 mmol/L) to optimize the reaction conditions. Each experiment was conducted in duplicate.

3. Results and discussion

3.1. SEM images and X-ray microanalysis of the catalysts

Fig. 1 shows SEM imagines of FeY (a and b) and FeZSM-5 (c and d) acquired from two kinds of synthesis methods. The zeolites appeared as conglomerate of irregular polyhedra, each of approximately 0.4–1.0 μm. No differences are observed in surface morphologies between the original and Fe-containing zeolites derived from different synthesis methods. The surface is smooth without any obvious deposit of iron species. This implies that iron species distributed mainly homogeneously into the micropores of zeolites, which is thought to be benefit for the stability and activity of the catalysts.

Crystalline phases of FeY_{ie} and $FeZSM-5_{co}$ calcined at 250, 350, 450 and 550 °C were observed using powder XRD analysis (Fig. 2) [20]. The peak intensity of ferrites and iron oxides are quite low. This is because that most iron species might distribute inside the cage structures of zeolites that cannot be reached by X-ray.

Calcinations significantly changed Fe speciation on FeY_{ie} (Fig. 2a). Only FeO was detected in the sample without calcination, and sekaninaite ($Fe_2Al_4Si_5O_{18}$) occurred in FeY_{ie}^{250}. In FeY_{ie}^{350} and FeY_{ie}^{450}, only sekaninaite was found, while in FeY_{ie}^{550}, α-Fe_2O_3 and Fe_3O_4 presented beside FeO and sekaninaite. The crystalline phases of immobilized irons on $FeZSM-5_{co}$ were all chlorite (Al–Fe–SiO_2–O) in spite of calcinated or not (Fig. 2b). However, with the increasing of calcination temperature, ZSM-5 itself was found to be dehydrated and dealuminated from $H_{1.61}Si_{94.22}Al_{1.78}O_{192} \cdot H_2O_{241}$ to $Si_{96}O_{192}$.

XPS survey and high-resolution surface scans for Fe 2p were obtained for the catalysts. The results of binding energies and atomic ratios are summarized in Table 1. The atomic ratio of Fe

Table 1
Binding energies (eV) and atomic ratios of the catalysts obtained by XPS

Samples	Binding energies (eV)		Atomic ratios	
	Si	Fe $2p_{3/2}$	Fe/Si	Fe(II)/Fe(III) (%/%)
FeY_{ie}	101.1 (68%)	710.8 (59%)	0.83	100/0
	104.1 (32%)	712.8 (42%)		
FeY_{ie}^{250}	101.1 (71%)	710.7 (44%)	0.80	55.8/44.2
	104.0 (29%)	712.7 (56%)		
FeY_{ie}^{350}	101.1 (69%)	711.2 (56%)	0.82	43.8/56.2
	103.7 (31%)	713.6 (44%)		
FeY_{ie}^{550}	101.1 (67%)	710.5 (31%)	0.84	10.5/89.5
	103.6 (33%)	713.2 (69%)		
$FeZSM-5_{co}$	101.3 (52%)	711.1 (46%)	0.78	46.3/53.7
	104.6 (48%)	713.3 (54%)		
$FeZSM-5_{co}^{450}$	101.2 (100%)	710.3 (49%)	0.76	48.9/51.1
		711.8 (51%)		
$FeZSM-5_{co}^{550}$	101.4 (58%)	710.8 (36%)	0.77	75.9/24.1
	104.2 (42%)	713.6 (64%)		

The values in parentheses represent the relative percentages of the peak components.
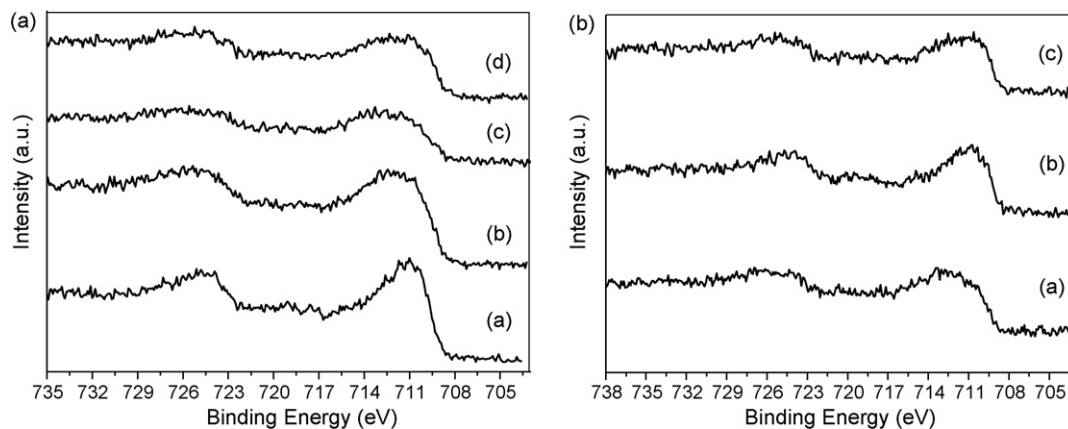
Fig. 3. Fe 2p XP-spectra of (a) FeY$_{ie}$ and (b) FeZSM-5$_{co}$ samples, which were (a) FeY$_{ie}$, (b) FeY$_{ie}^{250}$, (c) FeY$_{ie}^{350}$ and (d) FeY$_{ie}^{550}$ in left figure (a), and were (a) FeZSM-5$_{co}$, (b) FeZSM-5$_{co}^{450}$ and (c) FeZSM-5$_{co}^{550}$ in right figure (b).

to Si was very high (>0.75), but the actual iron-loading content was below 1% of the catalyst's dry weight. These indicate that the majority of immobilized Fe species on zeolites are located near the surface of the samples. Thus, together with the results from SEM, which indicates that no obvious surface Fe species layer could be seen, and very low peak intensity of Fe species by XRD, we draw a conclusion that iron species distributed mainly into the cage structures of zeolites' near surface.

Fe 2p$_{3/2}$ peak at approximately 707 eV corresponds to Fe^0 [21,22]. So, it is clear that no Fe^0 appeared in all samples. The over lapping peaks for Fe(II) and Fe(III) were observed in 710–713 eV range, indicating the simultaneous existence of ferrous or ferric sulfate and the formation of ferrous or ferric oxides on zeolites.

Fe 2p XP-spectra of FeY$_{ie}$ without calcination presents a broad band at approximately 711 eV (Fig. 3a), corresponding to FeSiO$_3$ and FeSO$_4 \cdot 7H_2O$ [22]. After calcination, Fe$_3$Al(SiO$_4$)$_3$ and FeSO$_4 \cdot 7H_2O$ were detected in FeY$_{ie}^{250}$. FeSO$_4$ and Fe(OH)O occurred in FeY$_{ie}^{350}$, Fe$_2$(SO$_4$)$_3$ and Fe$_3$O$_4$ presented in FeY$_{ie}^{550}$. These results imply that, ferrous species were oxidized to form a layer of Fe$_3$O$_4$ near the surface of the zeolites along with the increasing of calcination temperatures. It agrees with the results of XRD analysis. Fe 2p XP-spectra of FeZSM-5$_{co}$ without calcination also presents a broad band at about 712 eV (Fig. 3b), which corresponds to Fe$_2$(SO$_4$)$_3$ and FeSO$_4 \cdot 7H_2O$. After calcination, FeO and Fe(OH)O occurred in FeZSM-5$_{co}^{450}$, FeSO$_4$ and Fe$_3$O$_4$ were detected in FeZSM-5$_{co}^{550}$. Similar to FeY$_{ie}$, the oxidation of iron species formed a Fe$_3$O$_4$ layer finally.

3.2. Influence of synthesis method

Decolorization kinetics of 250 mg/L KN-R by 50 mmol/L H$_2$O$_2$ and 4.0 g/L the catalyst were examined at initial pH of 2.5. At the same time, decolorization by 15 mg/L Fe(II) ions was also observed (Fig. 4). The data within the first 20 min were used for kinetic correlation according to pseudo first-order equation [ln(C/C_0) = $-k_a t$] [7,8], and the apparent first-order rate constant (k_a) are listed in Table 2. The catalytic activities follow the order of FeZSM-5$_{co}$ > FeY$_{ie}$ > FeZSM-5$_{ie}$ > Fe(II) > FeY$_{co}$. FeZSM-5$_{co}$ has the highest KN-R decolorization capacity, whose k_a is
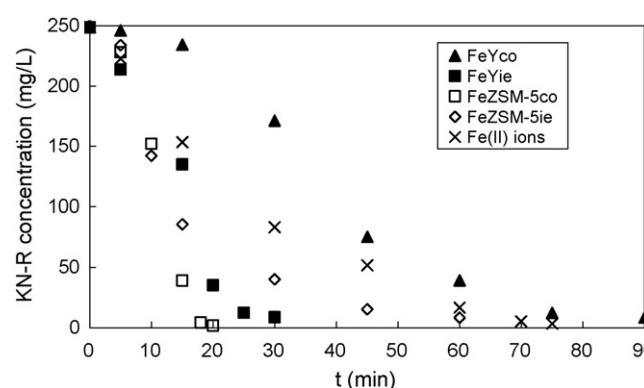

Fig. 4. KN-R decolorization kinetics catalyzed by FeY/FeZSM-5 prepared by coprecipitation and ion-exchange methods (pH 2.50, KN-R 250 mg/L, H$_2$O$_2$ 50.0 mmol/L and catalyst dose 4.0 g/L or Fe(II) ions 15 mg/L).

1.8×10^{-1} 1/min, which is four times higher than homogeneous Fenton reactions catalyzed by 15 mg/L Fe(II) ions.

Fe-loading contents in FeZSM-5$_{co}$, FeY$_{ie}$ and FeY$_{co}$ are all approximately 65 mg/g, while in FeZSM-5$_{ie}$ is only 4.5 mg/g. The leakage of dissolved iron ions from FeY and FeZSM-5 during decolorization was a little high in the first run (about 11.0–12.0 mg/g). However, after the third run, Fe leaching was already below 0.5 mg/g and 90% majority of the catalytic capacity remained. Hence, FeY$_{ie}$ and FeZSM-5$_{co}$ are better from the view of both catalytic activity and stability, and were used for further studies.

Table 2
Pseudo first-order rate constant of KN-R decolorization

Catalyst	Dosage	k_a (1/min)[a]	R^{2} [b]
Fe(II) ion	15.0 mg/L	3.7×10^{-2} [c]	0.9974
FeY$_{co}$	4.0 g/L	1.9×10^{-2}	0.9837
FeY$_{ie}$	4.0 g/L	1.4×10^{-1}	0.9948
FeZSM-5$_{co}$	4.0 g/L	1.8×10^{-1}	0.9983
FeZSM-5$_{ie}$	4.0 g/L	1.0×10^{-1}	0.9998

[a] k_a: pseudo first-order rate constant of KN-R decolorization.

[b] R^2: correlation coefficient.

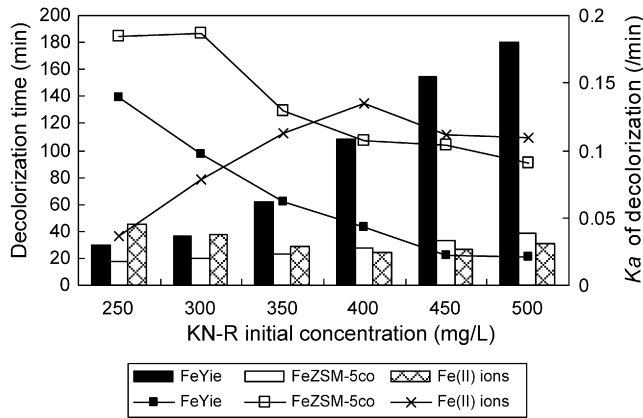[c] Under the condition of initial pH of 2.5, KN-R of 250 mg/L and H$_2$O$_2$ of 50.0 mmol/L.

Fig. 5. Influence of KN-R initial concentration on its decolorization (pH 2.50, H_2O_2 50.0 mmol/L and catalyst dose 4.0 g/L or Fe(II) ions 30 mg/L). Histograms describe the decolorization times (min) according to KN-R initial concentrations (mg/L). Decolorization time is the time when 95% dye KN-R was decolorized. And line charts present the apparent decolorization rate constants (/min) at various KN-R initial concentrations (mg/L).

3.3. Influence of KN-R initial concentration

Decolorizations of KN-R catalyzed by FeY_{ie} and $FeZSM-5_{co}$ under different KN-R initial concentrations of 250, 300, 350, 400, 450 and 500 mg/L were studied (Fig. 5). Decolorization catalyzed by 30 mg/L Fe(II) ions was done as a comparison. With the increasing of KN-R initial concentration, k_a of KN-R decolorization catalyzed by FeY_{ie} and $FeZMS-5_{co}$ decreased, and their decolorization efficiency was higher than Fe(II) ions only when KN-R initial concentration was <300 mg/L. When KN-R initial concentration was 500 mg/L, FeY_{ie} had k_a of only 2.0×10^{-2} 1/min, hence, FeY_{ie} was unsuitable for the treatment of high concentration dye wastewater compared to $FeZSM-5_{co}$.

The decline of catalytic efficiency with the increasing of KN-R initial concentration could be attributed to interface reaction processes. KN-R molecules need to be adsorbed onto zeolites before they can contact with Fe(II)/Fe(III) active sites in the catalysts. Along the elevation of dye initial concentration, the percentage of dye molecules which could be absorbed on zeolites decreased. In addition, the intermediate products of KN-R oxidation might compete for the limited adsorption sites with KN-R molecules, which blocked their interactions with Fe(II)/Fe(III) active sites. Hence, dosage of heterogeneous catalysts is an important factor that should be considered when applying this technology to the treatment of wastewaters of different chemical oxygen demand (COD) loadings.

3.4. Influence of catalyst dose

At pH 2.5, decolorizations of 250 mg/L KN-R catalyzed by FeY_{ie} and $FeZSM-5_{co}$ at different doses (2.0, 4.0 and 8.0 g/L) were examined with 50 mmol/L H_2O_2 to evaluate the influence of catalyst dosage. Fenton decolorization processes by 3.0–40.0 mg/L Fe(II) ions were observed for comparison (Fig. 6). KN-R decolorization apparent rate constant (k_a) reached the maximum of 4.0×10^{-2} 1/min when dissolved Fe(II) was higher than 15.0 mg/L. The excessive addition
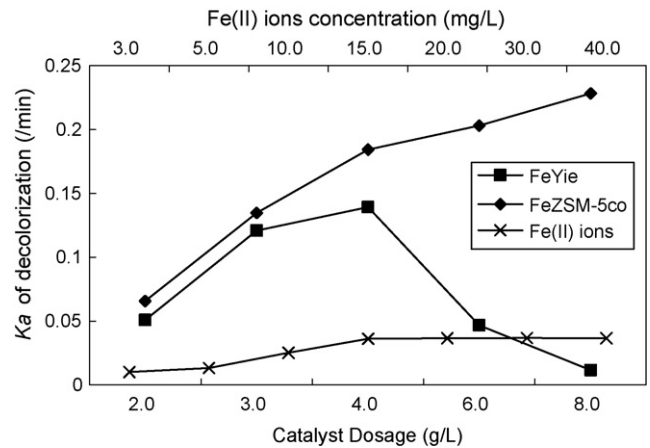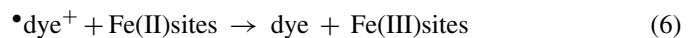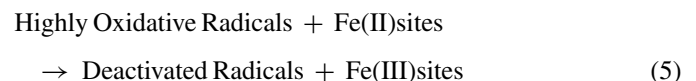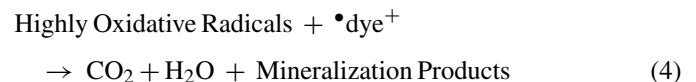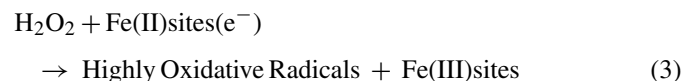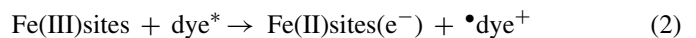

Fig. 6. Influence of initial catalyst dose on KN-R decolorization (pH 2.50, KN-R 250 mg/L and H_2O_2 50.0 mmol/L).

of FeY_{ie} resulted in lower decolorization efficiency, and its highest k_a of 1.4×10^{-1} 1/min was achieved at the dose of 4.0 g/L. For $FeZSM-5_{co}$, k_a increased continuously and reached 2.3×10^{-1} 1/min at the dose of 8.0 g/L.

To explain this, the main reaction mechanism is described (Eqs. (1)–(6)) according to references [7,8,23,24]:

$$dye + h\nu \rightarrow dye^* \tag{1}$$

$$Fe(III)sites + dye^* \rightarrow Fe(II)sites(e^-) + {}^\bullet dye^+ \tag{2}$$

$$\begin{aligned} &H_2O_2 + Fe(II)sites(e^-) \\ &\quad \rightarrow \text{Highly Oxidative Radicals} + Fe(III)sites \end{aligned} \tag{3}$$

$$\begin{aligned} &\text{Highly Oxidative Radicals} + {}^\bullet dye^+ \\ &\quad \rightarrow CO_2 + H_2O + \text{Mineralization Products} \end{aligned} \tag{4}$$

$$\begin{aligned} &\text{Highly Oxidative Radicals} + Fe(II)sites \\ &\quad \rightarrow \text{Deactivated Radicals} + Fe(III)sites \end{aligned} \tag{5}$$

$${}^\bullet dye^+ + Fe(II)sites \rightarrow dye + Fe(III)sites \tag{6}$$

Eqs. (1)–(4) describe the formation of highly oxidative radicals and the degradation processes of the dye, and Eqs. (5) and (6) describe the quenching of highly oxidative radicals and the deactivation of the free radical intermediate of the dye. When the dosage of heterogeneous catalysts was low (2.0–4.0 g/L), increasing catalyst dosage provided more active catalytic sites of Fe(II)/Fe(III) species to enhance decolorization (Eqs. (3) and (4)). However, when catalyst dosage continued to increase, superficial Fe(II) sites, which can catch highly oxidative radicals, also rapidly increased. Compared to organic chemicals, inorganic reducible Fe(II) species has much greater rate to capture and consume oxidative radicals (such as for $^\bullet OH$, $k \approx 4.0 \times 10^8$ L/(mol s)) [7,8,23,24]. The excessive Fe(II) sites would mainly react as capture agents for highly oxidative radicals, and themselves were transformed to Fe(III) (Eq. (5)). KN-R decolorization was consequently suppressed. In addition, during the electron transmission processes by iron compounds, the

cation dye free radical with a lost electron can capture electron from Fe(II) species, and lost its activity (Eq. (6)). These two anti-efficiency reactions possibly occupied the dominant position, and led to lower dye decolorization efficiency at 8.0 g/L FeY$_{ie}$.

For FeZSM-5$_{co}$, the tendency was a little different. FeZSM-5$_{co}$ had a higher adsorption capacity (10.0 mg/g for 250 mg/L KN-R) compared with FeY$_{ie}$ (only 3.7 mg/g). Hence, majority of Fe(II)/Fe(III) sites on ZEM-5 might be occupied by the activated dye molecules, and anti-efficiency reactions (Eqs. (5) and (6)) could not play a leading role even when FeZSM-5$_{co}$ was increased to 8.0 g/L. However, the enhancement of decolorization was slight when FeZSM-5$_{co}$ dose increased from 4.0 to 8.0 g/L, the optimal catalyst dosage was chosen at 4.0 g/L from the view of cost.

3.5. Influence of initial solution pH

In order to evaluate the influence of initial solution pH, the decolorization of 250 mg/L KN-R under the conditions of 50 mmol/L H$_2$O$_2$ and 4.0 g/L catalyst was examined, as solution pH was adjusted from 2 to 11 (Fig. 7). With the elevation of initial solution pH, the catalytic efficiency decreased dramatically, and no significant decolorization could be observed above pH 3.0. Acidic condition was needed for this heterogeneous catalytic dye decolorization. This is consistent with the proved opinion that the optimum pH of Fenton oxidation mostly falls in the pH range of 2.5–3.5 [24,25].

pH can influence the oxidation efficiency via several pathways [6,23–25]. Firstly, low pH favors $^\bullet$OH generation. Secondly, since pKa of HO$_2^\bullet$ is 4.8, the equilibrium is shifted towards HO$_2^\bullet$ at acidic pH [25], which can help to avoid the invalid consumption of Fe(II) by $^\bullet$O$_2^-$. Thirdly, pH strongly affects the oxidation of Fe(II) to Fe(III) [6]. Fe(II) tends to be oxidized and formed Fe(III) oxohydroxides at close to neutral pH, and its availability is strongly limited. Finally, the oxidation potential of highly oxidative radicals decreases with increasing pH [26]. $^\bullet$OH has oxidation potential of 2.65–2.80 V at pH 3.0, while only 1.90 V at pH 7.0 as a weaker oxidant. On the other hand, leaching of irons increased dramatically (histograms in
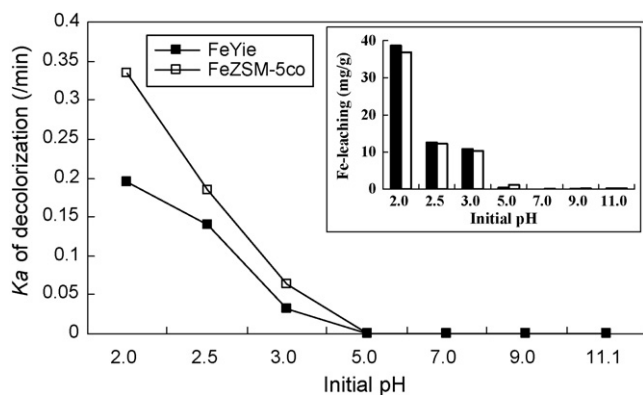
Fig. 7) at low pH, especially <2.0. Therefore, pH of 2.5 was considered the most suitable.

3.6. Activity and stability of the catalysts after calcination

Under pH of 2.50, H$_2$O$_2$ of 50.0 mmol/L, and catalyst dosage of 4.0 g/L, the decolorization of 250 mg/L KN-R was measured using FeY$_{ie}$ and FeZSM-5$_{co}$ calcined for 2 h at 250, 350, 450 and 550 °C, respectively (Fig. 8). KN-R decolorization apparent rate constant (k_a) catalyzed by FeY$_{ie}$ decreased obviously after calcinations. Meanwhile, XPS analysis (Fig. 3) showed that, above half of the ferrous species on FeY$_{ie}$ were oxidized by thermal treatments. Therefore, ferrous species could be deduced more important as the active centers on FeY$_{ie}$.

Decolorization was enhanced after FeZSM-5$_{co}$ calcinated at some temperatures, and FeZSM-5$_{co}^{450}$ (the number in the superscript represents calcination temperature, and the same below) had the highest k_a of 2.4 × 10^{-1} 1/min. The immobilized iron on FeZSM-5$_{co}$ (XRD in Fig. 2) was all chlorite (Al–Fe–SiO$_2$–O), and the data of XPS (Fig. 3) suggested no decline in the percentage of Fe(II) species on FeZSM-5$_{co}$ during the thermal treatments. However, FeZSM-5$_{co}$ was found to be dealuminated after calcination (XRD in Fig. 2), which might affect its decolorization capacity.

Si/Al molar ratio of zeolites has remarkable effects on the catalytic activity of zeolites-based catalysts [27,28]. Aluminum incorporated in the framework of zeolites results in Brønsted acidity, while extra-framework aluminum (or more accurately aluminum oxyhydroxides) results in Lewis acidity. Incomplete dealumination may transfer the framework aluminum to extra-framework aluminum, which prompts Lewis acidity. Zeolites with more Lewis acid sites favor the oxidation of molecules which cannot enter pore system. Moreover, dealumination of zeolites could provide a more hydrophobic surface, which is benefit for the adsorption and oxidation of hydrophobic molecules [27–29]. Therefore, the catalytic activity of FeZSM-5$_{co}$ increased after thermal treatments, and FeZSM-5$_{co}^{450}$ had the highest KN-R decolorization efficiency in the present work.
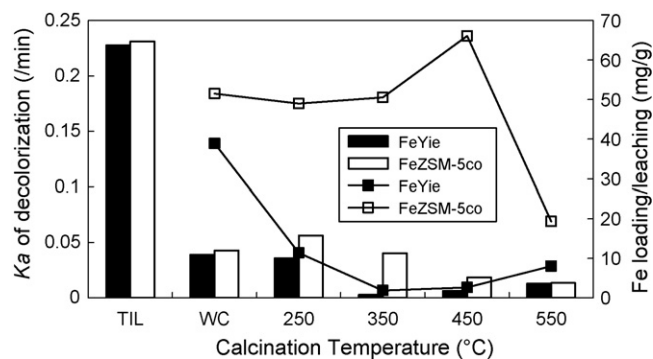

Fig. 7. Effect of solution initial pH on KN-R decolorization catalyzed by FeY$_{ie}$/FeZSM-5$_{co}$ (KN-R 250 mg/L, H$_2$O$_2$ 50.0 mmol/L and catalysts dose 4.0 g/L).

Fig. 8. Influence of calcination temperatures on KN-R decolorization catalyzed by FeY$_{ie}$/FeZSM-5$_{co}$ (pH 2.5, KN-R 250 mg/L, H$_2$O$_2$ 50.0 mmol/L and catalysts dose 4.0 g/L). TIL: total iron-loading content; WC: FeY$_{ie}$ and FeZSM-5$_{co}$ without calcination. Histograms describe the iron-loading content and the leaching of irons during decolorization according to calcination temperatures. And line charts present the apparent decolorization rate constants (/min) under different calcination temperatures.
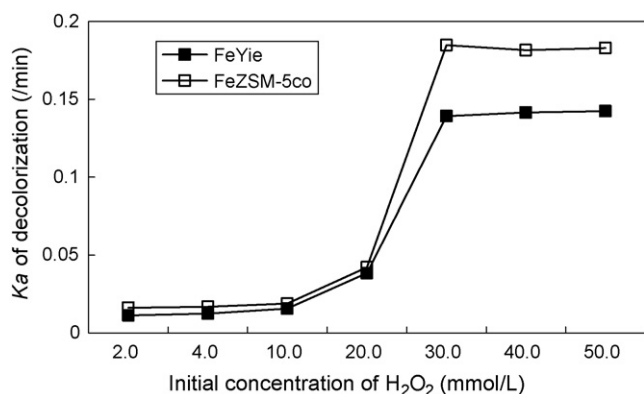
Fig. 9. Influence of H_2O_2 dose on KN-R decolorization catalyzed by FeY$_{ie}$/FeZSM-5$_{co}$ (pH 2.5, KN-R 250 mg/L and catalysts dose 4.0 g/L).

However, complete dealumination would lead to a reduction in total acidity on zeolites, which in turns would greatly decrease the catalytic activity [27,29]. When calcination temperature was increased to 550 °C, the catalytic activity of FeZSM-5$_{co}$ decreased obviously (Fig. 8), because ZSM-5 zeolite itself has been completely dealuminated to $Si_{96}O_{192}$.

The stabilities of FeY$_{ie}$ and FeZSM-5$_{co}$ after calcination are shown in histograms of Fig. 8. Except FeZSM-5$_{co}^{250}$, FeY$_{ie}$ and FeZSM-5$_{co}$ became more stable after calcination and FeY$_{ie}^{350}$ was the most. Thus, according to the decolorization efficiency and stability, FeZSM-5$_{co}^{450}$ was the best choice for KN-R decolorization.

3.7. Effect of initial H_2O_2 concentration

Under pH of 2.50, 250 mg/L KN-R was decolorized by 4.0 g/L catalysts using 2, 4, 10, 20, 30, 40 and 50 mmol/L H_2O_2, respectively (Fig. 9). The results showed that KN-R decolorization was slow under low H_2O_2 dose of 4–10 mmol/L, with k_a less than 2.0×10^{-2} 1/min. When H_2O_2 dose was elevated to 30–50 mmol/L, k_a reached the maximums about 1.8×10^{-1} 1/min for FeZSM-5$_{co}$ and 1.4×10^{-1} 1/min for FeY$_{ie}$, and KN-R was decolorized above 95% within 30 min.

Regarding homogeneous Fenton-like reactions, with the increasing of H_2O_2 dose vs the catalyst dose, reaction efficiency presents the tendency of increasing first, then reducing, and the best dose ratio is about 4:1 ([H_2O_2]:[Fe] mg/L:mg/L) [18,29]. In the present work, KN-R decolorization efficiency nearly did not change when the ratio of oxidant to catalyst ranging from 4:1 to 7:1, which means an easy control of the oxidation reactions compared to conventional Fenton-like processes. The optimal dose ratio between H_2O_2 and catalyst was chosen at 4:1 from the view of cost.

4. Conclusions

Fe-containing zeolites, FeY and FeZSM-5, were synthesized in this study, and their surface chemical-states and structures were investigated by SEM, XRD and XPS. Catalytic activities of the catalysts were examined using KN-R as a model organic chemical. Generally, the heterogeneous Fe catalysts had the similar or better catalytic activity as dissolved Fe(II) ions. Synthesis methods influenced the catalytic activity obviously. The decolorization could only be achieved at pH < 3.0, and initial dye concentration, catalyst and H_2O_2 doses influenced decolorization dynamics. The optimum conditions for KN-R decolorization were chosen as pH of 2.5, 4.0 g/L catalyst and 30 mmol/L H_2O_2. FeZSM-5$_{co}$ was better than FeY$_{ie}$ in term of catalytic efficiency and stability (measured by total dissolved Fe ions in reaction solutions) after calcinations. FeZSM-5$_{co}^{450}$ was the best for the heterogeneous catalytic dye decolorization.

Acknowledgment

References

[1] H. Katsumata, S. Kawabe, S. Kaneco, T. Suzuki, K. Ohta, Degradation of bisphenol A in water by the photo-Fenton reaction, J. Photochem. Photobiol. A 162 (2004) 297–305.

[2] R.F.P. Nogueira, A.G. Trovó, D. Modé, Solar photodegradation of dichloroacetic acid and 2. 4-dichlorophenol using an enhanced photo-Fenton process, Chemosphere 48 (2002) 385–391.

[3] X.J. Lv, Y.M. Xu, K.L. Lv, G.C. Zhang, Photo-assisted degradation of anionic and cationic dyes over iron(III)-loaded resin in the presence of hydrogen peroxide, J. Photochem. Photobio A: Chem. 173 (2005) 121–127.

[4] M.M. Cheng, W.H. Ma, J. Li, Y.P. Huang, J.C. Zhao, Y.X. Wen, Y.M. Xu, Visible-light-assisted degradation of dye pollutants over Fe(III)-loaded resin in the presence of H_2O_2 at neutral pH values, Environ. Sci. Technol. 38 (2004) 1569–1575.

[5] D. Gumy, P. Fernandez-Ibanez, S. Malato, C. Pulgarin, O. Enea, J. Kiwi, Supported Fe/C and Fe/Nafion/C catalysts for the photo-Fenton degradation of Orange II under solar irradiation, Catal. Today 101 (2005) 375–382.

[6] J. Lei, C.S. Liu, F.B. Li, X.M. Li, S.G. Zhou, T.X. Liu, M.H. Gu, Q.T. Wu, Photodegradation of orange I in the heterogeneous iron oxide-oxalate complex system under UVA irradiation, J. Hazard. Mater. 137 (2006) 1016–1024.

[7] J.X. Chen, L.Z. Zhu, Heterogeneous UV-Fenton catalytic degradation of dyestuff in water with hydroxyl-Fe pillared bentonite, Catal. Today 126 (2007) 463–470.

[8] J.X. Chen, L.Z. Zhu, Catalytic degradation of Orange II by UV-Fenton with hydroxyl-Fe-pillared bentonite in water, Chemosphere 65 (2006) 1249–1255.

[9] F.B. Li, X.Z. Li, X.M. Li, T.X. Liu, J. Dong, Heterogeneous photodegradation of bisphenol A with iron oxides and oxalate in aqueous solution, J. Colloid Interface Sci. 311 (2007) 481–490.

[10] S. Parra, L. Henao, E. Mielczarski, J. Mielczarski, P. Albers, E. Suvorova, J. Guindet, J. Kiwi, Synthesis, testing, and characterization of a novel Nafion membrane with superior performance in photoassisted immobilized Fenton catalysis, Langmuir 20 (2004) 5621–5629.

[11] D.O. Trong, D.D. Giscard, C. Danumah, S. Kaliaguine, Perspectives in catalytic applications of mesostructured materials, Appl. Catal. A: Gen. 222 (2001) 299–357.

[12] M. Ziolek, Catalytic liquid-phase oxidation in heterogeneous system as green chemistry goal-advantages and disadvantages of MCM-41 used as catalyst, Catal. Today 90 (2004) 145–150.

[13] M. Noorjahan, V.D. Kumari, M. Subrahmanyam, L. Panda, Immobilized Fe(III)-HY: an efficient and stable photo-Fenton catalyst, Appl. Catal. B 57 (2005) 291–298.

[14] M. Neamtu, C. Zaharia, C. Catrinescu, A. Yediler, M. Macoveanu, A. Kettrup, Fe-exchanged Y zeolite as catalyst for wet peroxide oxidation of

reactive azo dye Procion Marine H-EXL, Appl. Catal. B: Environ. 48 (2004) 287–294.

[15] V.R. Rani, M.R. Kishan, S.J. Kulkarni, K.V. Raghavan, Immobilization of metalloporphyrin complexes in molecular sieves and their catalytic activity, Catal. Commun. 6 (2005) 531–538.

[16] E.V. Kuznetsova, E.N. Savinov, L.A. Vostrikova, V.N. Parmon, Heterogeneous catalysis in the Fenton-type system FeZSM-5/H$_2$O$_2$, Appl. Catal. B: Environ. 51 (2004) 165–170.

[17] N.H. Phu, T.T.K. Hoa, N.V. Tan, H.V. Thang, P.L. Ha, Characterization and activity of Fe-ZSM-5 catalysts for the total oxidation of phenol in aqueous solutions, Appl. Catal. B: Environ. 34 (2001) 267–275.

[18] C.L. Hsueh, Y.H. Huang, C.C. Wang, C.Y. Chen, Degradation of azo dyes using low iron concentration of Fenton and Fenton-like system, Chemosphere 58 (2005) 1409–1414.

[19] USEPA, Phenanthroline Method, Standard Methods for the Examination of Water and Wastewater, 3500-Fe B.

[20] M.J. Wilson, A Handbook of Determinative Methods in Clay Mineralogy, Chapman and Hall, New York, 1987.

[21] G.A. Bukhtiyarova, V.I. Bukhtiyarov, N.S. Sakaeva, V.V. Kaichev, B.P. Zolotovskii, XPS study of the silica-supported Fe-containing catalysts for deep or partial H$_2$S oxidation, J. Mol. Catal. A-Chem. 158 (2000) 251–255.

[22] D. Briggs, M.P. Seah (Eds.), Practical Surface Analysis—Auger and X-ray Photoelectron Spectroscopy, vol. 1, second ed., Wiley Interscience, 1990.

[23] C. Walling, A. Goosen, Mechanism of the ferric ion catalyzed decomposition of hydrogen peroxide—effect of organic substrates, J. Am. Chem. Soc. 95 (1973) 2987–2991.

[24] J. De Laat, H. Gallard, Catalytic decomposition of hydrogen peroxide by Fe (III) in homogeneous aqueous solution: mechanism and kinetic modeling, Environ. Sci. Technol. 33 (1999) 2726–2732.

[25] A.A. Burbanoa, D.D. Dionysioua, M.T. Suidana, T.L. Richardson, Oxidation kinetics and effect of pH on the degradation of MTBE with Fenton reagent, Water Res. 39 (2005) 107–118.

[26] G.V. Buxton, C.L. Greenstock, W.P. Helman, A.B. Ross, Critical review of rate constants for reactions of hydrated electrons, hydrogen atoms and hydroxyl radicals ($^\bullet$OH/$^\bullet$O$^-$) in aqueous solution, J. Phys. Chem. Ref. Data 17 (1988) 513–886.

[27] M. Neamtu, C. Catrinescu, A. Kettrup, Effect of dealumination of iron(III)-exchanged Y zeolites on oxidation of Reactive Yellow 84 azo dye in the presence of hydrogen peroxide, Appl. Catal. B: Environ. 51 (2004) 149–157.

[28] S. Letaief, B. Casal, P. Aranda, M.A. Martin-Luego, E. Ruiz-Hitzky, Fe-containing pillared clays as catalysts for phenol hydroxylation, Appl. Clay Sci. 22 (2003) 263–277.

[29] L. Liu, M.J. Cheng, D. Ma, G. Hu, X.L. Pan, X.H. Bao, Synthesis, characterization, and catalytic properties of MWW zeolite with variable Si/Al ratios, Micropor. Mesopor. Mater. 94 (2006) 304–312.